

# $\pi$ -Stacking Functionalization of Carbon Nanotubes through Micelle Swelling\*\*

Cyrielle Roquelet,<sup>[a]</sup> Jean-Sébastien Lauret,<sup>\*[a]</sup> Valérie Alain-Rizzo,<sup>[b]</sup> Christophe Voisin,<sup>[c]</sup> Romain Fleurier,<sup>[d]</sup> Morgan Delarue,<sup>[a]</sup> Damien Garrot,<sup>[a]</sup> Annick Loiseau,<sup>[d]</sup> Philippe Roussignol,<sup>[c]</sup> Jacques A. Delaire,<sup>[b]</sup> and Emmanuelle Deleporte<sup>[a]</sup>

We report on a new, original and efficient method for  $\pi$ -stacking functionalization of single-wall carbon nanotubes. This method is applied to the synthesis of a high-yield light-harvesting system combining single-wall carbon nanotubes and porphyrin molecules. We developed a micelle-swelling technique that leads to controlled and stable complexes presenting an efficient energy transfer. We demonstrate the key role of

the organic solvent in the functionalization mechanism. By swelling the micelles, the solvent helps the non-water-soluble porphyrins to reach the micelle core and allows a strong enhancement of the interaction between porphyrins and nanotubes. This technique opens new avenues for the functionalization of carbon nanostructures.

## 1. Introduction

Molecular engineering of functionalized nanomaterials is a subject of intensive research in connection to a wide range of applications.<sup>[1]</sup> Such complexes aim at combining the unique properties of nano-objects and the wide tunability of the properties of organic molecules. Especially complexes presenting charge or energy transfer are intensively investigated for biology<sup>[1–3]</sup> or optoelectronics<sup>[4–7]</sup> applications. For instance, fluorescence energy transfer (FRET) has been used to monitor structural rearrangements in proteins<sup>[2]</sup> or to enhance the excitation transfer in dye-sensitized solar cells.<sup>[4]</sup> In this context, due to their unique transport properties and especially their large carrier mobility, single-wall carbon nanotubes (SWNTs) are of particular interest for use in organic photovoltaic devices.<sup>[5,8–13]</sup>

Excitation transfer between  $\pi$ -stacked porphyrin molecules and carbon nanotubes was demonstrated very recently.<sup>[14,15]</sup> The main advantage of  $\pi$ -stacking functionalization is that the electronic structure of nanotubes, and therefore their optical and transport properties, are hardly perturbed. In contrast, covalent functionalization is known to alter the mobility of carriers and to quench the nanotube luminescence.<sup>[16]</sup> On the other hand,  $\pi$ -stacking functionalization performances are quite poor regarding the yield of functionalization, the reproducibility and the stability of the suspensions. These difficulties are due to the weakness of the interactions involved in  $\pi$ -stacking functionalization and become problematic for scaling up a controlled process.

Herein, we report on the synthesis of controlled and stable SWNT/porphyrin complexes in micelles showing efficient energy transfer. The samples are obtained from aqueous suspensions of individual nanotubes in sodium cholate (SC) micelles. Transmission electron microscopy (TEM) combined with electron energy-loss spectroscopy (EELS) demonstrate the presence of tetraphenylporphyrin (TPP) molecules in the area of nanotubes. We investigate the functionalization process by

means of optical absorption spectroscopy (OAS) of suspensions of various concentrations and solvent/water volume ratios. We point out the crucial role of the organic solvent that acts as a vector for the insertion of the porphyrin molecules into the micelle core. Finally, by means of photoluminescence excitation (PLE) experiments, we demonstrate an efficient energy transfer from the excited porphyrin to the nanotube.

## 2. Results and Discussion

### 2.1. Structural Characterization

In a first approach, the composition of the SWNT/porphyrin suspensions is investigated by TEM. Figure 1a shows a typical area where we identify the presence of individual nanotubes

[a] C. Roquelet, Dr. J.-S. Lauret, M. Delarue, Dr. D. Garrot, Prof. E. Deleporte  
Laboratoire de Photonique Quantique et Moléculaire  
Institut d'Alembert, CNRS, ENS Cachan,  
61 avenue du Président Wilson, 94235 Cachan Cedex (France)  
Fax: (+33) 147405567  
E-mail: lauret@lpqm.ens-cachan.fr

[b] Dr. V. Alain-Rizzo, Prof. J. A. Delaire  
Laboratoire de Photophysique et Photochimie Supramoléculaires et  
Macromoléculaires  
Institut d'Alembert, CNRS, ENS Cachan  
61 avenue du Président Wilson, 94235 Cachan Cedex (France)

[c] Dr. C. Voisin, Prof. P. Roussignol  
Laboratoire Pierre Aigrain  
Ecole Normale Supérieure, UPMC, Université Denis Diderot, CNRS  
24 rue Lhomond, 75005 Paris (France)

[d] Dr. R. Fleurier, Prof. A. Loiseau  
Laboratoire d'Etude des Microstructures  
ONERA, CNRS, 29 avenue de la division Leclerc, 92322 Chatillon (France)

[\*\*] Synthesis of Complexes for Energy Transfer

Supporting information for this article is available on the WWW under  
<http://dx.doi.org/10.1002/cphc.201000067>.

embedded in surfactant molecules. Nanotubes are difficult to distinguish because their contrast is shrouded by the amorphous contrast of the surfactant molecules. However as shown by the arrows in Figure 1 a, one can distinguish the presence of straight lines with a spacing close to 1 nm, which is consistent with the nanotube contrast.<sup>[17]</sup>

Additional EELS measurements have been recorded for the whole area depicted in Figure 1 a. The corresponding spectrum is displayed in Figure 1 b. An absorption edge close to 400 eV typical of the N–K edge is observed, indicating the presence of nitrogen. This element is never observed in pristine nanotube. Furthermore, the fine structure of the absorption edge displays two features identified as a  $\pi^*$  peak at 397 eV and a  $\sigma^*$  peak at

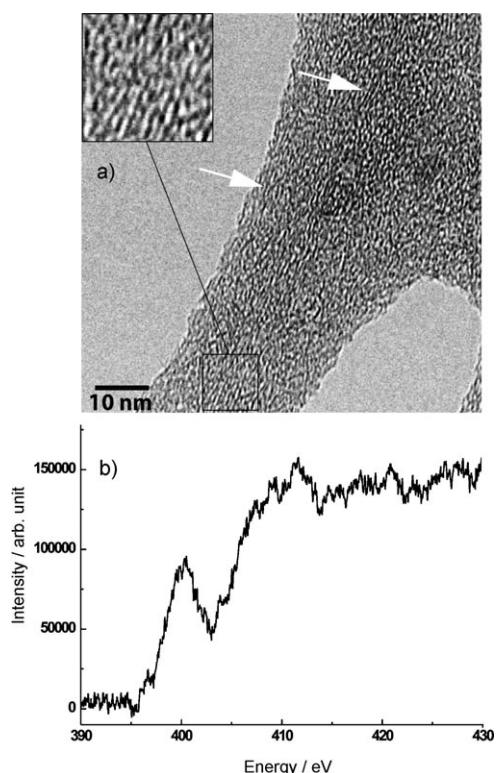


**Figure 1.** a) TEM image of typical grids prepared from the SWNT/TPP suspensions. The arrows indicate single nanotubes embedded in surfactant. b) EELS spectrum after subtraction of the continuum background, recorded on area shown in image (a).

400 eV. These features are characteristic of nitrogen bonded to carbon atoms in  $sp^2$  configuration, which is the case in the tetraphenylporphyrin (TPP) molecule used herein. Since no other component of the suspension is expected to contain nitrogen, this band is interpreted as the signature of porphyrin molecules. Thus, porphyrin molecules are present in the close vicinity of the nanotubes.

## 2.2. Optical Properties

### Optical Absorption

Figure 2 displays the optical absorption spectrum (OAS) of the SWNT/TPP suspension together with the ones of a suspension of pure SWNTs and a suspension of pure TPP, both in SC micelles. The TPP suspension shows the Soret band at 420 nm and the four weaker Q bands in the 500–700 nm region.

The OAS of SWNTs consists in a group of lines in the 1000 nm region corresponding to the  $S_{11}$  (lowest) transitions in semi-conducting nanotubes. Each line in this group stems from a given  $(n,m)$  chiral family. Additional lines near 600 nm

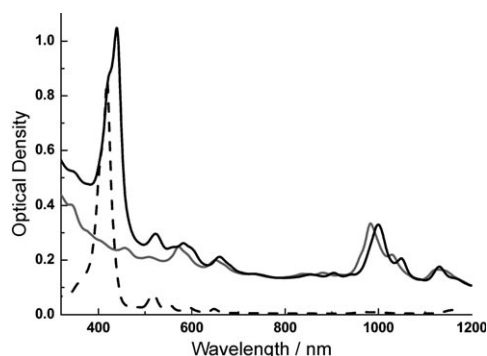


**Figure 2.** Optical absorption spectra of TPP molecules (dashed line, rescaled for clarity), of a reference suspension of SWNT (grey solid curve) and of SWNT/TPP complexes (black solid curve) all of them embedded in micelles of sodium cholate in a pH 8 buffer.

and at smaller wavelengths come from  $S_{22}$  transitions superimposed to the onset of  $M_{11}$  transitions in metallic nanotubes. The background in OAS mainly stems from light scattering and is subtracted when analyzing the line amplitudes.

The OAS of the SWNT/TPP suspension shows a band at 438 nm with a shoulder at 420 nm. These lines are attributed to the Soret absorption band of TPP encased in micelles (at 420 nm, in agreement with the OAS of pure TPP in micelles) and of TPP stacked on nanotubes (438 nm). This 18 nm red-shift of the Soret band when porphyrin molecules are  $\pi$ -stacked on the nanotubes is consistent with previous observations<sup>[14,18]</sup> and is related to a conformation change of the TPP molecules. The presence of these two bands shows that the suspension contains both pure TPP molecules encased in micelles and TPP stacked on nanotubes in micelles. The absorption features around 1000 nm are consistent with  $S_{11}$  absorption lines in semi-conducting nanotubes. We note, however, a 7 nm red-shift compared to the reference SWNT suspension. This bathochromic shift is due to the presence of TPP close to the nanotubes and to the resulting interaction.

### Control of the Functionalization

In contrast with previous reports on SWNT/TPP stacking, the key of our work is to provide a reliable method to produce

samples of controlled and reproducible quality. The control of the process is investigated by studying the functionalization yield as a function of amount of TPP. Figure 3 shows the OAS of suspensions made from the same reference SWNT suspension mixed with a fixed volume of dichloromethane (DCM)

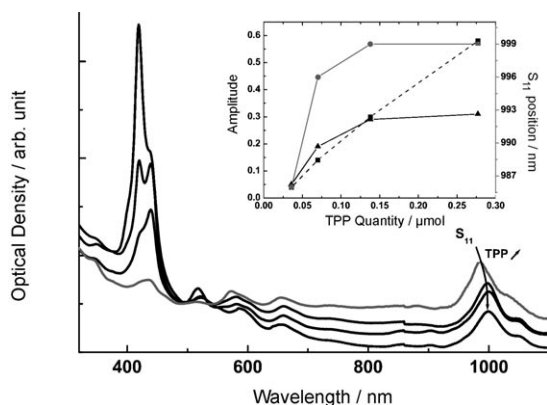


**Figure 3.** Optical absorption spectra of SWNT/TPP complexes for different concentrations of porphyrin with a DCM/water volume ratio of 34%: 0.04  $\mu\text{mol}$  (light grey), 0.07  $\mu\text{mol}$  (grey), 0.14  $\mu\text{mol}$  (dark grey) and 0.27  $\mu\text{mol}$  (black). The curves are vertically translated to match at 490 nm (background correction). Inset: Amplitude of the band at 420 nm (dashed line) and at 438 nm (black line) in function of the quantity of porphyrin; Shift of the  $S_{11}$  band (grey line) in function of the quantity of porphyrin.

(2.5 mL of SWNT suspension with 0.85 mL of DCM, volume ratio 34%) containing a quantity of TPP ranging from 0.04  $\mu\text{mol}$  up to 0.28  $\mu\text{mol}$ . The four curves are arbitrary shifted (background correction) in order to match at 490 nm and to facilitate the comparison of the peak amplitudes. For low TPP concentrations (light grey and grey curves), the band at 438 nm (stacked TPP) is higher than the one at 420 nm (free TPP). The two bands have the same intensity for a TPP quantity of 0.14  $\mu\text{mol}$  (dark grey curve). For a larger amount of TPP, the band at 420 nm becomes predominant. The amplitude of each band as a function of TPP concentration is plotted in the inset of Figure 3. The free TPP band (420 nm) grows regularly with the initial TPP concentration whereas the amplitude of the stacked TPP band reaches a plateau above 0.14  $\mu\text{mol}$ .

These results are interpreted as follows. At low TPP concentration, TPP molecules are preferentially  $\pi$ -stacked on SWNTs rather than encased alone in micelles, therefore the amplitude of the 438 nm band is higher than the one at 420 nm. For an amount of TPP larger than 0.14  $\mu\text{mol}$ , no more porphyrin can stack onto the nanotubes and the TPP molecules mostly aggregate in micelles due to the excess of SC. The amplitude of the 438 nm band is saturated while the one at 420 nm grows regularly with the TPP quantity (inset of Figure 3). The position of the  $S_{11}$  band of SWNTs is another way to track the stacking of TPP onto SWNTs. For a small amount of TPP, the  $S_{11}$  band (near 1000 nm) is identical to the one in the reference SWNT suspension. Most of the nanotubes are not functionalized. This band progressively red-shifts with increasing TPP concentration. Above the saturation threshold ( $\sim$ 0.14  $\mu\text{mol}$ ), the position

of  $S_{11}$  reaches a plateau and most of the nanotubes are functionalized (grey curve in the inset of Figure 3).

Importantly, the absorption amplitude of the  $S_{11}$  band is almost identical in both the SWNT/TPP and the reference SWNT suspensions. This point shows that only few nanotubes are lost in the process. The increase in TPP quantity only affects the functionalization degree of nanotubes. This is due to the stability of micelle suspensions of nanotubes. The use of such a stable starting material is the key for the reproducibility and control of our method, in contrast to previous attempts where soluble TPP molecules were used for both solubilization and functionalization of SWNTs.<sup>[14]</sup>

### Functionalization mechanism

In view of further developments of this technique, a good description of the functionalization mechanism is needed. The SWNT/TPP complex is hydrophobic and is thus expected to stay in the organic core of the micelles in water suspensions. However, the formation mechanism of such a complex from pre-existing SWNT micelles and non-water-soluble TPP is less straightforward, since TPP molecules have to diffuse through water to reach the core of the micelles. We show that an organic solvent can act as a vector and help TPP molecules to penetrate into the micelles. The control parameter is the DCM/water volume ratio, which drives the exchange area between the two immiscible liquids during the sonication process. The OAS of SWNT/TPP suspensions for various volumes of DCM but with a constant quantity of TPP (0.14  $\mu\text{mol}$ ) is displayed in Figure 4.<sup>[19]</sup> For a DCM/water volume ratio of  $\sim$ 2% no functionalization is observed (light grey curve in Figure 4). For a volume ratio of  $\sim$ 7%, both the 420 nm and 438 nm Soret bands are observable but with a weak amplitude (grey curve). For an increasing DCM/water volume ratio up to 27% (dark grey and black curves), both bands rise, meaning that both the stacking of porphyrin onto nanotubes and the formation of TPP aggregates in micelles become efficient. Bearing in mind that the quantity of TPP is kept constant, this reveals the central role of DCM in the functionalization mechanism.

Wang et al. have shown that water-immiscible organic solvents allow the micelle hydrophobic core surrounding the SWNT to swell.<sup>[20]</sup> The authors have mixed a micelle suspension of nanotubes with immiscible organic solvents. The presence of the organic solvent inside the micelle is investigated by means of optical spectroscopy. Typical solvatochromic shifts are observed in the photoluminescence (PL) spectra and interpreted as a signature of nanotubes coated by the solvent. The organic solvent evaporates over time and after several hours the initial optical spectra are recovered, showing the reversibility of the mechanism. The solvent/water ratio in ref. [20] is of the order of 50%, close to that used in our studies (34%) for optimal synthesis conditions. Therefore, we can confidently extend their conclusions to our work. When mixing the SWNT suspension with the TPP solution, DCM swells the sodium cholate micelle and therefore acts as a vector for the interaction between the porphyrin molecules and the nanotubes. This mechanism is schematically depicted in the upper panel of

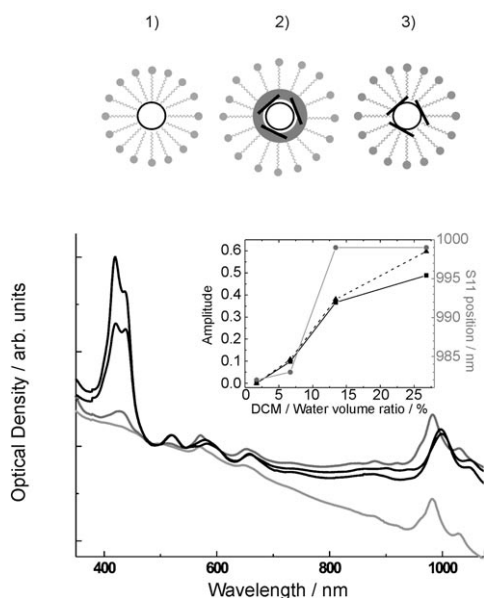


**Figure 4.** Top: Swelling of the micelle by the dichloromethane (dark grey) leading to the functionalization of the nanotubes (black line) by the porphyrin molecules (grey stick). Bottom: Optical absorption spectra of SWNT/TPP complexes for different DCM/water volume ratios, but with the same amount of TPP (0.14  $\mu\text{mol}$ ). Light grey: 2%, Grey: 7%, Dark grey: 13% and Black: 27%. Inset: Amplitude of the band at 420 nm (dashed line) and at 438 nm (black line) in function of the DCM/water volume ratio; Shift of the  $S_{11}$  band (grey line) in function of the DCM/water volume ratio.

Figure 4. The starting material is a nanotube encased in a micelle (step 1). After addition of the DCM solution of TPP, the DCM swells the hydrophobic core of the micelle bringing porphyrin molecules in contact with the nanotube (step 2). As described in reference,<sup>[20]</sup> DCM rapidly evaporates: TPP molecules stack onto the nanotubes (step 3) and the new complex remains in the micelle core.

Optical absorption spectra recorded just after and several hours after the synthesis do not show any noticeable change. We can therefore conclude that the samples investigated herein correspond to step 3 of Figure 4.

This micelle core swelling by organic solvents as a way to enhance the interaction between  $\pi$ -conjugated molecules and nanotubes is promising and should open new avenues for nanotube functionalization.

## 2.2. Stability

Spectroscopic measurements of SWNT/TPP suspensions were recorded at different time delays (up to several months) after the synthesis and no noticeable evolution could be detected. An important point is that the PL signal is stable for months (see Figure S1, Supporting Information), which is the major improvement of our method compared with previous reports.<sup>[14,15]</sup> Furthermore, the PL intensity of the SWNT/TPP suspension corresponding to the emission of nanotubes is on the same order of magnitude as that of the reference SWNT suspension. It is one order of magnitude higher than for suspensions obtained with the soluble TPP stacking method.<sup>[14]</sup> In

contrast with the earlier work, this observation confirms that our micelle-based synthesis ensures that most of the nanotubes remain in the final product.

## 2.3. Energy Transfer

In this section we probe the interaction between the porphyrin and the nanotube by means of photoluminescence experiments. The PL spectra of the SWNT reference suspension and of the SWNT/TPP suspension are almost identical, except that all bands are red-shifted by nearly 20 nm, as already mentioned for absorption spectra.

The PLE spectrum of the reference SWNT suspension detected at 984 nm (Figure 5 grey curve) consists of a broad line near 560 nm. This couple of PL/PLE wavelengths or equivalently  $S_{11}$  and  $S_{22}$  energies allows us to identify a specific chiral family, namely the (6,5) family.<sup>[21]</sup>

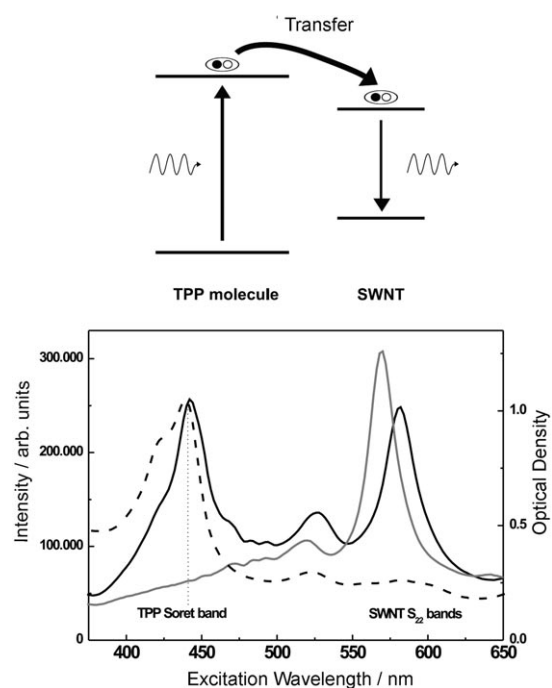


**Figure 5.** Top: Excitonic levels and energy transfer mechanism. Bottom: PLE spectra of the SWNT suspension (grey) and of the SWNT/TPP suspension (black) detected at 984 nm and 1007 nm respectively. Dashed line: optical absorption spectrum of the SWNT/TPP suspension.

The PLE spectrum of SWNT/TPP complexes (black curve) strongly contrasts with that of the reference SWNT suspension. The PLE spectrum shows a strong additional line at 440 nm. This line corresponds to the absorption of stacked TPP (dashed curve). This PLE peak is the signature of the energy transfer from the photosensitized porphyrin to the nanotube.<sup>[14,15]</sup> When photons are absorbed by a stacked porphyrin, they give rise to photons emitted by the nanotube (as depicted in the upper panel of Figure 5). The line at 580 nm is clearly the  $S_{22}$  line of the nanotubes. Interestingly, this line is red-shifted by about 10 nm in comparison to the reference SWNT suspension.

This result is similar to the shift observed for the  $S_{11}$  lines. Therefore, we conclude that this effect arises from a dielectric screening of excitons and not from a strain-induced band-shift (as observed for some surfactants<sup>[22,23]</sup>) that would result in opposite shifts for  $S_{22}$  and  $S_{11}$  lines.<sup>[24]</sup>

Remarkably, the amplitudes of PLE lines corresponding to porphyrin Soret band and to  $S_{22}$  nanotubes transitions are of the same order of magnitude. This means that the number of photons emitted by the SWNTs is the same when the SWNTs are excited directly ( $S_{22}$  absorption) or through TPP absorption. We conclude that the energy transfer from the photo-sensitized porphyrin molecules to the nanotubes is very efficient. Nevertheless, further measurements are required in order to quantify precisely the transfer quantum yield.

### 3. Conclusions

We have developed a new method for  $\pi$ -stacking functionalization of carbon nanotubes by organic molecules. An organic solvent is used to swell the micelle surrounding the nanotube and to bring the organic molecules onto the nanotube in the core of the micelle. This new method allows the production of controlled, reproducible and stable suspensions of SWNT/TPP complexes. These complexes show an efficient energy transfer from the photosensitized porphyrin molecules to the nanotubes, confirming the potential of this system for light-harvesting applications. This physico-chemical functionalization method combines the advantages of  $\pi$ -stacking functionalization with a remarkable stability of the obtained complexes. This is a significant step towards scaling up a controlled process and designing functional nanodevices. Finally, this method is neither specific to nanotubes nor to porphyrins and can therefore be generalized to a wide range of nano-objects and dye molecules.

### Experimental Section

**Preparation of SWNT/TPP Suspensions:** The nanotubes used herein are synthesized by the CoMoCAT process<sup>[25]</sup> and produced by SouthWest Nanotechnologies. The mean diameter of these tubes is about 0.8 nm. The nanotube suspensions are prepared by adding raw nanotubes at 0.15 mg·mL<sup>-1</sup> in a pH 8 Normadose buffer (10<sup>-2</sup> M, Prolabo) plus 2 wt% of sodium cholate (Sigma-Aldrich). The mixture is sonicated for 1.5 h with an ultrasonic tip and ultracentrifuged at 120 000 g for 1 h. Then, the supernatant is drawn out. It consists in a suspension of isolated nanotubes.<sup>[26]</sup>

Nanotube functionalization is achieved by mixing the nanotube suspension with a solution of porphyrin in DCM, in this case tetraphenylporphyrin purified twice by column chromatography. After adding the TPP solution to the nanotube suspension, the mixture is sonicated for 2 h with an ultrasonic tip. The sample is placed in a thermostat at 12 °C during sonication. The phase corresponding to DCM in excess is removed and the sample is centrifuged at 3000 g for 10 min. The supernatant is drawn out and a suspension of SWNT/porphyrin complexes is obtained.

**Spectroscopic Measurements:** Optical absorption spectra are recorded with a spectrophotometer (Lambda 900 Perkin-Elmer). A laser diode emitting at 532 nm is used as excitation source for

photoluminescence experiments. The signal is dispersed in a spectrograph (Spectrapro 2300i, Roper Scientific) and detected by an IR CCD (OMAV, PI Acton). A UV/Vis Xe lamp and a monochromator (Spectrapro 2150i, Roper Scientific) are used as tunable light source for the photoluminescence excitation experiments.

**TEM Measurements:** TEM images and EELS are recorded using a Libra200 transmission electron microscope at an accelerating voltage of 200 kV. A three times diluted suspension is used for preparing deposits on TEM grids. Then, the grid is rinsed with water to remove the excess sodium cholate.

### Acknowledgements

The authors are grateful to D. E. Resasco for providing the CoMoCAT nanotubes produced by SouthWest Nanotechnologies. LPQM, PPSM and LPA are "Unités mixtes" de recherche associées au CNRS (UMR8537, UMR8531, UMR8551). This work was supported by the GDR-E "nanotube" (GDRE2756), the grant C'Nano IdF EPONAD from the Région Ile de France and ANR grant CEDONA. Upon submitting this manuscript, we became aware of the related work published by W. C. Chen et al.<sup>[27]</sup>

**Keywords:** energy transfer · functionalization · light-harvesting systems · nanotubes · porphyrins

- [1] A. E. Nel, L. Mdlar, D. Velegol, T. Xia, E. M. V. Hoek, P. Somasundaran, F. Klaessig, V. Castranova, M. Thompson, *Nat. Mater.* **2009**, *8*, 543.
- [2] J. W. Taraska, M. C. Puljung, N. B. Olivier, G. E. Flynn, W. N. Zagotta, *Nat. Methods* **2009**, *6*, 532.
- [3] B. Saccà, R. Meyer, C. M. Niemeyer, *Nat. Protocols* **2009**, *4*, 271.
- [4] B. E. Hardin, E. T. Hoke, P. B. Armstrong, J. H. Yum, P. Comte, T. Torres, J. M. J. Fréchet, Md. K. Nazeeruddin, M. Grätzel, M. D. McGehee, *Nat. Photonics* **2009**, *3*, 406.
- [5] C. Ehli, C. Oelsner, D. M. Guldi, A. Mateo-Alonso, M. Prato, C. Schmidt, C. Backes, F. Hauke, A. Hirsch, *Nat. Chem.* **2009**, *1*, 243.
- [6] S. H. Park, A. Roy, S. Beaupré, S. Cho, N. Coates, J. S. Moon, D. Moses, M. Leclerc, K. Lee, A. J. Heeger, *Nat. Phot.* **2009**, *3*, 297.
- [7] R. B. Ross, C. M. Cardona, D. M. Guldi, S. G. Sankara-Narayanan, M. O. Reese, N. Kopidakis, J. Peet, B. Walker, G. C. Bazan, E. Van Keuren, B. C. Holloway, M. Drees, *Nat. Mater.* **2009**, *8*, 208.
- [8] S. Campidelli, B. Ballesteros, A. Filoramo, D. Díaz Díaz, G. de La Torre, T. Torres, G. M. Aminur Rahman, C. Ehli, D. Kiessling, F. Werner, V. Sgobba, D. M. Guldi, C. Cioffi, M. Prato, J. P. Bourgoin, *J. Am. Chem. Soc.* **2008**, *130*, 11503.
- [9] C. Ehli, G. M. Aminur Rahman, N. Jux, D. Balbinot, D. M. Guldi, F. Paolucci, M. Marcaccio, D. Paolucci, M. Melle-Franco, F. Zerbetto, S. Campidelli, M. Prato, *J. Am. Chem. Soc.* **2006**, *128*, 11222.
- [10] M. Alvaro, P. Atienzar, P. De La Cruz, J. L. Delgado, V. Troiani, H. Garcia, F. Langa, A. Palkar, L. Echegoyen, *J. Am. Chem. Soc.* **2006**, *128*, 6626.
- [11] T. Hasobe, S. Fukuzumi, P. V. Kamat, *J. Phys. Chem. B* **2006**, *110*, 25477.
- [12] G. M. Aminur Rahman, A. Troeger, V. Sgobba, D. M. Guldi, N. Jux, D. Balbinot, M. N. Tchoul, W. T. Ford, A. Mateo-Alonso, M. Prato, *Chem. Eur. J.* **2008**, *14*, 8837.
- [13] S. Giordani, J. F. Colomer, F. Cattaruzza, J. Alfonsi, M. Meneghetti, M. Prato, D. Bonifazi, *Carbon* **2009**, *47*, 578.
- [14] G. Magadur, J. S. Lauret, V. Alain-Rizzo, C. Voisin, Ph. Roussignol, E. Deleporte, J. A. Delaire, *ChemPhysChem* **2008**, *9*, 1250.
- [15] J. P. Casey, S. M. Bachilo, R. B. Weisman, *J. Mater. Chem.* **2008**, *18*, 1510.
- [16] M. A. Herranz, N. Martin, S. Campidelli, M. Prato, G. Brehm, D. M. Guldi, *Angew. Chem.* **2006**, *118*, 4590; *Angew. Chem. Int. Ed.* **2006**, *45*, 4478.
- [17] P. Lambin, A. Loiseau, M. Monthieux, J. Thibault, in *Understanding Carbon Nanotubes* (Eds.: A. Loiseau, P. Launois, P. Petit, S. Roche, J.-P. Salvetat), Springer, Berlin, **2006**.

- [18] S. Cambré, W. Wenseleers, J. Caronulin, S. VanDoorslaer, A. Fonseca, J. B. Nagy, E. Goovaerts, *ChemPhysChem* **2008**, *9*, 1930.
- [19] As shown in the previous section, this amount of TPP is sufficient for a full functionalization of all the SWNTs.
- [20] R. K. Wang, W. C. Chen, D. K. Campos, K. J. Ziegler, *J. Am. Chem. Soc.* **2009**, *131*, 16330.
- [21] S. M. Bachilo, M. S. Strano, C. Kittrell, R. H. Hauge, R. E. Smalley, R. B. Weisman, *Science* **2002**, *298*, 2361.
- [22] O. Kiowski, S. Lebedkin, F. Hennrich, S. Malik, H. Rösner, K. Arnold, C. Sürgers, M. M. Kappes, *Phys. Rev. B* **2007**, *75*, 075421.
- [23] Y. Ohno, S. Iwasaki, Y. Murakami, S. Kishimoto, S. Maruyama, T. Mizutani, *Phys. Status Solidi B* **2007**, *244*, 4002.
- [24] S. Berger, F. Iglesias, P. Bonnet, C. Voisin, G. Cassabois, J. S. Lauret, C. Delalande, Ph. Roussignol, *J. Appl. Phys.* **2009**, *105*, 094323.
- [25] G. Lolli, L. Zhang, L. Balzano, N. Sakulchaicharoen, Y. Tan, D. E. Resasco, *J. Phys. Chem. B* **2006**, *110*, 2108.
- [26] M. J. O'Connell, S. M. Bachilo, C. B. Huffman, V. C. Moore, M. S. Strano, E. H. Haroz, K. L. Rialon, P. J. Boul, W. H. Noon, C. Kittrell, J. Ma, R. H. Hauge, R. B. Weisman, R. E. Smalley, *Science* **2002**, *297*, 593.
- [27] W. C. Chen, R. K. Wang, K. J. Ziegler, *ACS Appl. Mater. & Int.* **2009**, *1*, 1821; *Int.* **2009**, *1*, 1821.

---

Received: January 27, 2010

Published online on April 6, 2010